SUPPORTING INFORMATION

Insights into the involvement of spliceosomal mutations in myelodysplastic disorders from analysis of SACY-1/DDX41 in *Caenorhabditis elegans*

Tatsuya Tsukamoto,*[,1] Micah D. Gearhart,*[,1] Seongseop Kim,*[,1,2] Gemechu Mekonnen,* Caroline A. Spike,* and David Greenstein*[,3]

*Department of Genetics, Cell Biology and Development, University of Minnesota, Minneapolis, Minnesota 55455, USA

[1]These authors contributed equally to this work.

[2]Present address: OriGene Technologies Inc., 9620 Medical Center Drive, Suite 200, Rockville, MD 20850

[3]Corresponding author: David Greenstein, Department of Genetics, Cell Biology, and Development, University of Minnesota, 4-208 MCB, 420 Washington Avenue SE, Minneapolis, MN 55455. Tel: 612-624-3955; FAX: 612-626-6140. E-mail: green959@umn.edu

Contents:

Table S1 *C. elegans* strains used in this study.

Strain	Genotype
N2	Wild type, Bristol isolate
BS553[a]	*fog-2(oz40)* V
CA1200	*ieSi57[eft-3p::TIR1::mRuby::unc-54 3'utr + Cb unc-119(+)]* II; *unc-119(ed3)* III
CA1352	*ieSi64[gld-1p::TIR1::mRuby::gld-1 3'utr + Cb unc-119(+)]* II; *unc-119(ed3)* III
CB61	*dpy-5(e61)* I
CB2167	*dpy-5(e61) unc-13(e1091)* I
CB3778[a]	*tra-2(e2020)* II
CB3843	*fem-3(e1996)/unc-24(e138) dpy-20(e1282)* IV
DG2347	*acy-4(ok1806)* V*; tnEx37[acy-4(+) + sur-5::gfp]*
DG2873	*lin-41(n2914)* I/*hT2[bli-4(e937) let-?(q782) qIs48]* (I;III)
DG3430	*sacy-1(tn1385)* I
DG3485	*sacy-1(tm5503)* I; *tnEx159[gfp::tev::s-tag::sacy-1 + Cb unc-119(+)]*
DG3492	*sacy-1(tm5503)* I/*hT2[bli-4(e937) let-?(q782) qIs48]* (I;III)
DG3528	*sacy-1(tm5503)* I/*hT2[bli-4(e937) let-?(q782) qIs48]* (I;III); *fem-3(e1996)/unc-24(e138) dpy-20(e1282)* V
DG3611	*sacy-1(tm5503)* I; *unc-119(ed3)* III; *tnEx159[gfp::tev::s-tag::sacy-1 + Cb unc-119(+)]*
DG3628	*sacy-1(tn1385) unc-13(e51)* I; *fog-2(oz40)* V
DG3672	*gld-1(tn1478Mog)* I/*hT2[bli-4(e937) let-?(q782) qIs48]* (I;III)
DG3688	*sacy-1(tn1482)* I
DG3739	*sacy-1(tn1481)* I*; tnEx159[gfp::tev::s-tag::sacy-1 + Cb unc-119(+)]*
DG3768	*sacy-1(tm5503)* I; *unc-119(ed3) tnIs102[sacy-1p::gfp::tev::s-tag::sacy-1 + Cb unc-119(+)]* III
DG3700	*sacy-1(tn1385)* I/*hT2[bli-4(e937) let-?(q782) qIs48]* (I;III); *emb-4(sa44)/unc-51(e369)* V
DG3751	*sacy-1(tn1481)* I/*hT2[bli-4(e937) let-?(q782) qIs48]* (I;III); *fem-3(e1996)/unc-24(e138) dpy-20(e1282)* V
DG3787	*sacy-1(tn1480)* I

DG3789 *sacy-1(tn1385)* I; *glp-1(ar202)* III

DG3800[a] *sacy-1(tm5503)* I/*hT2[bli-4(e937) let-?(q782) qIs48]* (I;III); *tra-2(e2020)* II

DG3801[a] *sacy-1(tn1481)* I/*hT2[bli-4(e937) let-?(q782) qIs48]* (I;III); *tra-2(e2020)* II

DG3805 *sacy-1(tn1479)* I/*hT2[bli-4(e937) let-?(q782) qIs48]* (I;III)

DG3807 *sacy-1(tn1481)* I/*hT2[bli-4(e937) let-?(q782) qIs48]* (I;III)

DG3821 *sacy-1(tn1481)*/*sacy-1(tm5503)* I

DG3832 *sacy-1(tn1481)* I; *unc-119(ed3)* III; *tnEx159[gfp::sacy-1 unc-119(+)]*

DG3913 *lin-41(tn1541[gfp::tev::s-tag::lin-41])* I

DG4008 *lin-41(tn1541[gfp::tev::s-tag::lin-41]) sacy-1(tn1602)* I/*hT2[bli-4(e937) let-?(q782) qIs48]* (I;III)

DG4009 *lin-41(tn1541[gfp::tev::s-tag::lin-41]) sacy-1(tn1603)* I/*hT2[bli-4(e937) let-?(q782) qIs48]* (I;III)

DG4010 *lin-41(tn1541[gfp::tev::s-tag::lin-41]) sacy-1(tn1604)* I/*hT2[bli-4(e937) let-?(q782) qIs48]* (I;III)

DG4011 *lin-41(tn1541[gfp::tev::s-tag::lin-41]) sacy-1(tn1605)* I/*hT2[bli-4(e937) let-?(q782) qIs48]* (I;III)

DG4012 *lin-41(tn1541[gfp::tev::s-tag::lin-41]) sacy-1(tn1606)* I/*hT2[bli-4(e937) let-?(q782) qIs48]* (I;III)

DG4013 *lin-41(tn1541[gfp::tev::s-tag::lin-41]) sacy-1(tn1607)* I/*hT2[bli-4(e937) let-?(q782) qIs48]* (I;III)

DG4014 *lin-41(tn1541[gfp::tev::s-tag::lin-41]) sacy-1(tn1608)* I/*hT2[bli-4(e937) let-?(q782) qIs48]* (I;III)

DG4015 *lin-41(tn1541[gfp::tev::s-tag::lin-41]) sacy-1(tn1609)* I/*hT2[bli-4(e937) let-?(q782) qIs48]* (I;III)

DG4016 *lin-41(tn1541[gfp::tev::s-tag::lin-41]) sacy-1(tn1610)* I/*hT2[bli-4(e937) let-?(q782) qIs48]* (I;III)

DG4017 *lin-41(tn1541[gfp::tev::s-tag::lin-41]) sacy-1(tn1611)* I/*hT2[bli-4(e937) let-?(q782) qIs48]* (I;III)

DG4018 *lin-41(tn1541[gfp::tev::s-tag::lin-41]) sacy-1(tn1612)* I/*hT2[bli-4(e937) let-?(q782) qIs48]* (I;III)

DG4023 *sacy-1(tn1617)* I/*hT2[bli-4(e937) let-?(q782) qIs48]* (I;III)

DG4024	*sacy-1(tn1615)* I/*hT2[bli-4(e937) let-?(q782) qIs48]* (I;III)
DG4025	*sacy-1(tn1616)* I/*hT2[bli-4(e937) let-?(q782) qIs48]* (I;III)
DG4068	*sacy-1(tn1632[3xflag::PreScission protease site::gfp::tev::s-tag::sacy-1]) fog-1(q253*ts*)* I
DG4070	*sacy-1(tn1632[3xflag::PreScission protease site::gfp::tev::s-tag::sacy-1])* I
DG4700	*sacy-1(tn1880[aid::gfp::myc::sacy-1])* I; *ieSi64[gld-1p::TIR1::mRuby::gld-1 3'UTR + Cb unc-119(+)]* II
DG4703	*sacy-1(tn1880[aid::gfp::myc::sacy-1])* I; *ieSi57[eft-3p::TIR1::mRuby::unc-54 3'utr + Cb unc-119(+)]* II
DG4724	*sacy-1(tn1887)* I
DG4735	*sacy-1(tn1887) I; fog-2(oz40)* V
DG4750	*sacy-1(tn1887)* I*; acy-4(ok1806)* V*; tnEx37[acy-4(+) + sur-5::gfp]*
DG4757	*sacy-1(tn1887)* I; *glp-1(ar202)* III
DG4761	*sacy-1(tn1887) unc-13(e1091)* I
DG4762	*dpy-5(e61) sacy-1(tn1887)* I
DG4771	*sacy-1(tn1480) unc-13(e1091)* I
DG4774	*dpy-5(e61) sacy-1(tn1480)* I
DG4819	*sacy-1(tn1481)/tmC18* I*; her-1(hv1y101)* V
DG4825	*unc-13(e1091) sacy-1(tn1480)/sacy-1(tm5503)* I
FX30152	*tmC12[egl-9(tmIs1194) + pmyo-2::Venus]* V
FX30168	*tmC18[dpy-5(tmIs1236) + pmyo-2::mCherry]* I
GC833	*glp-1(ar202)* III
MT12853	*her-1(hv1y101)* V

[a]Male-female strain.

Table S2 Oligonucleotides used in this study.

Oligonucleotide name	Sequence
A. Oligonucleotides used for PCRs and sequencing of the indicated loci and to identify mutations and verify genotypes of animals	
*e2020*_F1	TCTACTCATATCTAATCGTCCACTCGACC
*fem-3*_F2	CTAATTCCAGCCCAATCCGGATCCGAATTG
*fem-3*_R2	TCTCCATGGCTAAACGATAGTGCTCAATAC
*GFP*_7215	GGCGATGGCCCTGTCCTTTTA
*GFP*_1094R	ACCTTCGGGCATGGCACT
*GFP*_F1	AGTCCTCCTCCCAGACAACCAC
*GFP*_R1	CACGGGTCTTGTAGTTTCCGTC
*gld-1*_F1	TCGTTAGATAAGCTAGATGAGCGAATCG
*gld-1*_F3	GATTATGGTCCGAGGAAAGGGATCAATG
*gld-1*_R2	GTTTTCTCTTCAGCTCGTCAGTTCCCTC
*gld-1*_R4	GGAAGATTCTACAGGGGTTAGCGTTAAG
*gld-1*_seq_F1	TGAGTTATGGAAAATCATCGATGGACAAG
*gld-1*_seq_F2	ATCCAACCTTCTCGGATCTAACGTCTTC
*gld-1*_seq_R1	GATTGGTTCTGTAGCTGTTGGAGAGAAC
*gld-1*_seq_R2	TGGCAACATGATGTATGGCACATGATTC
H27M09.1[a]_F1	AAATCAGCACTGGTCAAACCTATTGTAAG
*H27M09.1*_F2	TACTCCCAAAAGTTGTCATTCTTCAATTC
*H27M09.1*_F3	TTGTTTTACCGTTAGTTATGTTCTGTTTG
*H27M09.1*_F4	TCAAATCTTTGACCTGATCATTGAAATG
*H27M09.1*_F5	ACTGCTGGAAGATATATCACTTATCGTC
*H27M09.1*_F6	GATAAAGTTACACGTGGTGGAGGTCTC
*H27M09.1*_R1	GACAATCTGTGATGCGATGACCCAG
*H27M09.1*_R2	CTGGAAGTTCCTGCCCTGCTTC
*H27M09.1*_R3	ATTGAAGAATGACAACTTTTGGGAGTAG
*H27M09.1*_R4	TTAAACATGAAATAAATAGTACAATTCTGAC
*H27M09.1*_R5	CGGTGGAATATGATCACCTTCACAAC

*H27M09.1*_seq_F1	GTAGAATCCAATGCGACTTAAATATATAC
*H27M09.1*_seq_F2	GCAGTTGCTGAACTTACAAAAGGTG
*H27M09.1*_seq_F3	GCAACAGATGTTGCATCAAAAGGAC
*sa44*_F1	CCGACGTCGCCGTGCAGATTATCTC
*sa44*_R1	AAAAGTATCCGGCATTCTCACAAGTGTAC
*sa44*_seqF1	GGCCGAATCAACGTACGCTCATC
sacy-1 seq_F1	CTCTCCTTTTCTCGGCTACGATGCCACGAAAG
sacy-1 seq_R1	TCAGAAACCACCATCGTCGCCTCCACCTC
*tm5503*_F1	GTTATTGACGAATCAGAACGGCAATTAATG
*tm5503*_R1	CTTGTATCTGAATAGCTGTCGGTGTCAC
*tra-2*_F1	GTGGAGCATGTCCTTCCAGAAGAATATC
*tra-2*_R2	TTGTTTGTGCCTTTTCACCTACCAATTC

B. Oligonucleotides used for genome editing to generate double-stranded DNA repair templates or as single-stranded DNA repair templates

sacy-1 5HAF	CAATTTTTTTAAGTATCTTAAAAAGTAGAACAGAAAAATTCGTTTAGTATTC CGAAATGGACTACAAAGACCATGACGGTGATTATAAAGATCATGATATCGAT TACAAGGATGACGATGACAAGCTTGAAGTTCTTTTCCAAGGACCATCATCAG GAATGAGTAAAGGAGAAGAACTTTTCACTGGAGTTG
sacy-1 3HAR	CTTCCTCTTGAATTTTTCGCCGGCGGTCCT
sacy-1 AID5_F	CAAGTTCAATTTTTTTAAGTATCTTAAAAAGTAGAACAGAAAAATTCGTTTA GTATTCCGAAATGCCTAAAGATCCAGCCAAACCTCCGGCCAAGGC
sacy-1 AID3_R	CTTTCATTTCTTCCTCTTGAATTTTTCGCCGGCGGTCCTCATATTTTCGTCG CGCCGCTTCCACATCTGTGCTTCTCTTGTCATCGTCATCCTTGTAATCACGC TTGTCGTCG
sacy-1 GM1	TTTCTTATTTATTTTTCATAATTGAATTTTTATTTTCAGTTCATCGAATTGG TCGTACCGGACACTCGGGACGTAAAGGTCTCGCAACGACATTTATCAACAAA AAATCGGAGATGTCAGTGCTTTCCG

C. Oligonucleotides used to generate single-guide RNAs for genome editing

sacy-1 sgRNA1_F	TCTTGTCCGAAATGAGCACAGATG
sacy-1 sgRNA1_R	AAACCATCTGTGCTCATTTCGGAC
sacy-1 sgRNA7_F	TCTTGAGATTATGGAGACACAAGG
sacy-1 sgRNA7_R	AAACCCTTGTGTCTCCATAATCTC
sacy-1 sgRNA11_F	TCTTGCCGGACGTTCCGGACGGAA

sacy-1 sgRNA11_R	AAACTTCCGTCCGGAACGTCCGGC
sacy-1 sgRNA12_F	TCTTGTCGTACCGGACGTTCCGGA
sacy-1 sgRNA12_R	AAACTCCGGAACGTCCGGTACGAC

[a]*H27M09.1* is *sacy-1*.

Table S3. Spliceosomal proteins associated with SACY-1 using tandem affinity purification

		Protein Coverage (%)[a]	
		Experiment I	Experiment II
Protein		Tandem IP female background[b]	Tandem IP hermaphrodite background[b]
SACY-1	DDX41/Abstrakt/recruited to C-complex	78.9	76.5
Spliceosomal proteins	Human protein/Spliceosome subcomplex		
PRP-19	PRP19hPRP19/CDC5L complex[c]	62.0	55.5
MOG-2[d]	U2A'/17S U2 snRNP[c]	56.1	42.3
SKP-1	SNW1/SKIP/hPRP19/CDC5L-related complex	52.9	40.9
EMB-4, isoform b	Aquarius/KIAA0560/Intron-binding complex RNA helicase[c, e]	50.4	30.6
PRP-17	hPRP17/WD40-domain step 2	48.3	33.7

	factor[c, f]		
CYN-13	Cyclophilin E/PPIE/Intron-binding complex[e]	46.8	37.8
CDC-5L	CDC5L/hPRP19/CDC5L complex[c]	45.8	26.2
Y69A2AR.21	CCDC12/Recruited to B-complex[c]	45.6	52.1
RBM-22	RBM22/ hPRP19/CDC5L-related complex[c, g]	45.1	43.9
EFTU-2[d]	U5 116K[c]	45.1	37.2
ISY-1	hIsy1/Intron-binding complex[e]	40.8	34.8
PLRG-1	PLRG1/PRL1/hPRP19/CDC5L complex[c]	39.1	27.3
RBMX-2[d]	CGI-79/SNU17/IST3/hRes complex[c]	38.7	20.9
CYN-10	PPIL3b/peptidyl-prolyl isomerase recruited to C-complex[c]	37.9	23.6
RBM-25	RBM25/affects alternative splicing/putative U1 snRNP	37.5	25.8

	component		
RNP-6, isoform a	PUF60/U2AF65-related promotes alternative splicing[h]	37.2	49.3
SYF-2	GCIP p29/SYF2/Recruited to C-complex[c]	37.2	29.9
PRP-8	PRPF8/PRP8/U5 220K[i]	37.0	29.4
EMB-4, isoform a	Aquarius/KIAA0560/Intron-binding complex RNA helicase[c, d]	36.8	28.6
DDX-35	DDX35/DHX35/Recruited to C-complex[c]	36.8	19.8
SNRP-40.1	snRNP40/U5 40K[c]	36.6	27.5
RBM-39[d]	RBM39/protein recruited to A-complex[c]	35.9	31.0
CACN-1	Cactin/C-complex[c, j]	35.9	13.4
ACIN-1	Acinus/Exon junction complex[c]	35.2	13.1
M03F8.3	hSYF3/CRNKL1/hPRP19/CDC5L-related protein	35.0	24.3

ZK1098.1	PRP40/FBP11[k]	34.5	28.7
C50D2.5	SF3b14/SF3b6/17S U2 snRNP protein	33.3	8.7
SYF-1	hSyf1/Xab2/Intron-binding complex[e]	32.4	28.0
EMB-4, isoform e	Aquarius/KIAA0560/Intron-binding complex RNA helicase[c, e]	31.7	18.4
F33D11.10	EIF4A3/ Exon junction complex[c]	31.3	17.0
REPO-1	SF3a66/SF3A2/17S U2 snRNP protein[c, l]	30.6	5.9
Y54G2A.12	hPRP17/hCDC40/Step 2 factor	29.9	27.7
PNN-1	Pinin/Exon junction complex[c]	28.7	20.3
BCAS-2	Spf27/BCAS2/hPRP19/CDC5L complex[c]	28.6	20.2
EMB-4, isoform d	Aquarius/KIAA0560/Intron-binding complex RNA helicase[c, e]	28.3	27.9

RSP-7	p54 SR protein[m]	27.2	27.4
CWC-15	CCAP2/CWC15/hPRP19/CDC5L complex[c]	27.0	22.6
LET-858	KIAA1604/CWC22/Recruited to B-complex[c]	26.5	16.5
RSR-2	SRm300/SRRM2	24.0	21.2
MOG-3	CCDC49/CWC25/recruited to C-complex[n]	21.3	20.0
CYN-12	PPIL1/ peptidyl-prolyl isomerase/hPrp19/CDC5L-related protein	20.1	20.1
F25B4.5	PRPF39/PRP39/U1 snRNP auxiliary protein[o]	20.1	10.0
SNRP-40.2	U5 snRNP 40K[c]	19.6	16.0
C16C10.4	SAP18/Exon junction complex[c]	17.5	7.8
DDX-23	U5 snRNP 100K/PRP28[c]	17.1	7.5

R08D7.1	BUD13/hRes complex[c]	16.6	3.7
TEG-4	SF3b130/SF3B3/17S U2 snRNP[c]	14.9	8.8
SFTB-1[s]	SF3b155/SF3B1/17S U2 snRNP[c]	14.7	1.2
F53H1.1, isoform a	SF3b125/17S U2 snRNP[p]	14.5	3.4
RNP-6, isoform b	PUF60/U2AF65-related promotes alternative splicing[h]	13.6	20.3
PRPF-4, isoform a	PRP4 kinase[r]	12.5	7.1
RNP-3	U2B''/17S U2 snRNP[c]	12.4	12.4
F53H1.1, isoform e	SF3b125/17S U2 snRNP[p]	11.9	5.1
PRP-21	SF3a120/SF3A1/PRP21/17S U2 snRNP protein[c]	11.8	7.0
SNRP-200[d]	U5 200K[c]	11.1	7.7
SFTB-2	SF3b145/SF3B2/17S U2 snRNP[c]	10.1	1.5
RNP-5	RNPS1/EJC[c]	10.0	18.0

[a]Peptide coverage in a single gel slice assessed by mass spectrometry in the various SACY-1 purifications from DG4068 *sacy-1(tn1632[3x flag::PreScission::gfp::tev::s::sacy-1]) fog-1(q253)* extract and DG4070

sacy-1(tn1632) extract. Only proteins showing at least 10% coverage in the tandem immunopurification (IP) from the high-speed supernatant are shown. The complete data on which Table S3 is based, including filtering criteria, are presented in File S1.

[b]Experiments I and II utilized 515 mg and 280 mg total protein, respectively, from a high-speed supernatant for tandem IP.

[c]Bessonov *et al*. 2008.

[d]MOG-2, EFTU-2, RBMX-2, RBM-39, SFTB-1, TEG-4 and SNRP-200 are reported in Table S3 and not filtered out despite their low representation (14.2%, 4.4%, 3.6%, 6.9%, 2.0%, 1.1% and 4.5% coverage, respectively) in the LIN-41 tandem IP from high-speed supernatant (Tsukamoto *et al*. 2017) because they were reported as splicing factors. F33D11.10 is reported in Table S3 despite its low representation (10.3% coverage) in the OOC-5 tandem IP from high-speed supernatant (unpublished data) because it was reported as a splicing factor.

[e]De *et al.* 2015; Haselbach *et al*. 2018.

[f]Bertram *et al*. 2017.

[g]Zhang *et al*. 2017.

[h]Page-McCaw *et al*. 1999; Van Buskirk and Schüpbach 2002; Hastings *et al*. 2007.

[i]Grainger and Beggs 2005.

[j]Fica *et al*. 2019.

[k]Kao and Siliciano 1996.

[l]Keikhaee *et al*. 2014.

[m]Chaudhary *et al*. 1991; Longman *et al*. 2000.

[n]Fabrizio *et al*. 2009.

[o]Li *et al*. 2017.

[p]Will *et al*. 2002.

[q]Schneider *et al*. 2010.

Table S4. Spiceosomal proteins not reproducibly associated with SACY-1.

		Protein Coverage (%)[a]	
		Experiment I	Experiment II
Protein		Tandem IP female background[b]	Tandem IP hermaphrodite background[b]
SACY-1	DDX41/Abstrakt/recruited to C-complex	78.9	76.5
Spliceosomal proteins	Human protein/Spliceosome subcomplex		
Y66D12A.8	CXorf56/potential C-complex specific protein	30.7	0.0
SNR-3	D1/SMD1/Sm protein D1[c]	31.0	0.0
RBM-17	SPF45/RBM17/17S U2-related protein[c]	27.5	0.0
BUD-31	G10/BUD31/fSAP17hPRP19/CDC5L-related complex	25.2	0.0

T13H5.4	SF3a60/SF3A3/PRP9/17S U2 snRNP[c]	19.0	0.0
SAP-49	SF3b49/SF3b4/17S U2 snRNP[c]	16.2	0.0
MAG-1	Magoh/Exon junction complex[c]	15.8	0.0
K07C5.6	hSLU7/Step 2 factor	15.0	0.0
DDX-15	hPRP43/DDX15/17S U2-related[c]	11.1	0.0

[a]Peptide coverage in a single gel slice assessed by mass spectrometry in the various SACY-1 purifications from DG4068 *sacy-1(tn1632[3x flag::PreScission::gfp::tev::s::sacy-1]) fog-1(q253)* extract and DG4070 *sacy-1(tn1632)* extract. Only proteins showing at least 10% coverage a tandem immunopurification (IP) from the high-speed supernatant are shown. The complete data on which Table S4 is based are presented in File S1.

[b]Experiments I and II utilized 515 mg and 280 mg total protein, respectively, from a high-speed supernatant for tandem IP.

[c]Bessonov *et al*. 2008.

Table S5. Non-spliceosomal proteins associated with SACY-1 by tandem affinity purification.

		Protein Coverage (%)[a]	
		Experiment I	Experiment II
Protein		Tandem IP female background[b]	Tandem IP hermaphrodite background[b]
SACY-1	DDX41/Abstrakt/recruited to C-complex	78.9	76.5
FTN-2	Ferritin heavy chain	50.6	28.8
Y66D12A.9	Proteasome activator subunit 3/PSME3	42.3	43.6
KIN-3	Casein kinase 2 alpha subunit	36.1	23.3
LET-504	NF kappa B-activating protein/NKAP	31.6	32.3
D1037.1	NREBP/SON DNA-binding protein	28.8	19.1
R07E5.1	GPATCH1/ECGP	26.0	11.2

CIR-1[c]	CIR/CBF1-interacting corepressor protein	25.7	29.6
C37C3.1	SCAF11	24.0	17.0
XNP-1	ATRX	23.9	16.6
D1054.10	NA	22.9	17.0
F46G10.1	NA	19.7	17.4
MBF-1	Endothelial differentiation related factor/EDF1	19.2	12.8
C13F10.7	SREK1IP1	18.9	18.9
CDK-12	CDK12	18.2	18.2
K08E3.5	UGP2	18.1	15.5
RBPL-1	RBBP6 E3 ubiquitin ligase	17.8	9.1
W08G11.3	NA	16.7	15.1
T07F10.3	tRNA selenocysteine 1-associated protein 1	16.7	7.3

PRDX-2	Peroxiredoxin 2	16.4	11.4
NRDE-2	NRDE2	15.5	9.0
CCNK-1	CCNK/Cyclin K	14.3	7.9
Y67D2.7	SAP30 binding protein	13.5	5.4
C54C6.6	CFAP20	12.8	11.3
ULE-5	NA	12.7	16.0
Y37D8A.2	PLBD2	12.3	2.5
NARS-1	Asparaginyl amino-acyl tRNA synthetase	11.6	12.5
F33G12.2	WDR83	11.2	9.2
B0513.4	NA	10.8	10.8
CDK-11.1	CDK11A	10.2	2.8

[a]Peptide coverage in a single gel slice assessed by mass spectrometry in the various SACY-1 purifications from DG4068 *sacy-1(tn1632[3x flag::PreScission::gfp::tev::s::sacy-1]) fog-1(q253)* extract and DG4070 *sacy-1(tn1632)* extract. Only proteins showing at least 10% coverage in a tandem immunopurification (IP) from the high-speed supernatant are shown. Only proteins reproducibly associated with SACY-1 are shown. The complete data on which Table S5 is based are presented in File S1.

[b]Experiments I and II utilized 515 mg and 280 mg total protein, respectively, from a high-speed supernatant for tandem IP.

[c]CIR-1 was reported to be associated with MOG-3 (Kasturi *et al*. 2010).

Table S6. Association of spliceosomal proteins with SACY-1 at higher stringency

	Spectral Counts[a]		
	Experiment III	Experiment IV	Experiment V
Protein	300 mM KCl wash	1 M KCl wash	300 mM KCl wash with 5 µg/ml RNase A
SACY-1	181	176	161
Spliceosomal proteins			
PRP-8	61	14	7
RBM-39	43	44	42
EMB-4	36	24	3
SNRP-200	36	2	0
EFTU-2	30	13	13
TEG-4	29	0	0
SYF-1	26	14	7

ZK1098.1	23	6	3
RNP-6	22	21	29
F33D11.10	21	17	3
M03F8.3	21	10	5
CDC-5L	20	2	1
SFTB-1	19	0	6
PRP-17	17	4	1
DDX-35	14	18	19
PRP-19	14	7	5
RSP-7	13	7	4
CACN-1	13	4	18
MOG-3	12	5	4
ACIN-1	11	7	10
RBM-22	11	1	0

SNRP-40.1	11	0	0
CYN-13	10	11	11
PLRG-1	8	1	2
MOG-2	8	1	1
PRP-21	7	0	0
SKP-1	6	2	0
ISY-1	5	8	0
SYF-2	5	0	0
PRPF-4	4	13	36
LET-858	4	0	0
CYN-12	3	2	2
F53H1.1	3	0	9
C16C10.4	2	3	1
RBM-25	4	0	0

CWC-15	2	0	0
RNP-5	2	0	0

[a]The total number of peptides (spectral counts) observed for each protein in all gel slices as assessed by mass spectrometry in the various SACY-1 purifications from DG3768 *sacy-1(tm5503)* I; *unc-119(ed3) tnIs102[sacy-1p::gfp::tev::s-tag::sacy-1 + Cb unc-119(+)]* III. Small-scale single immunopurifications using a monoclonal anti-GFP monoclonal antibody were conducted using 80 mg of protein lysate. In addition to standard conditions (e.g., 300 mM KCl), higher stringency washes were conducted with 1 M KCl or 300 mM KCl containing 5 μg/ml RNase A. The bound proteins were cleaved from the affinity matrix using TEV protease and analyzed by mass spectrometry. Table S6 reports the data for the spliceosomal proteins reproducibly associated with SACY-1 in tandem affinity purifications (shown in Figure 1F and listed Table S3). Only proteins represented by at least 2 spectral counts under standard conditions (300 mM KCl) are listed. File S1 contains the complete dataset.

Table S7 Limiting *cacn-1(RNAi)* mimics *Y111B2A.25(RNAi)* in the *sacy-1(tn1385) reduction-of-function* genetic background.

RNAi[a]	Genotype	Sterile[b] (%)	Gamete degeneration[b] (%)	Embryonic lethal[c] (%)
L4440 (control)	Wild type	0 (n=338)	0 (n=338)	1 (n=674)
	sacy-1(tn1385)	0 (n=256)	0 (n=256)	1 (n=502)
Y111B2A.25	Wild type	22 (n=230)	1 (n=94)	84 (n=463)
	sacy-1(tn1385)	95 (n=272)	16 (n=110)	93 (n=42)
cacn-1 (1:1)	Wild type	100 (n=146)	45 (n=146)	ND
	sacy-1(tn1385)	100 (n=34)	100 (n=34)	ND
cacn-1 (1:10)	Wild type	99 (n=152)	11 (n=152)	ND
	sacy-1(tn1385)	100 (n=126)	75 (n=126)	ND
cacn-1 (1:50)	Wild type	22 (n=196)	2 (n=196)	95 (n=633)

	sacy-1(tn1385)	92 (n=166)	18 (n=166)	ND
cacn-1 (1:100)	Wild type	3 (n=144)	1 (n=144)	88 (n=629)
	sacy-1(tn1385)	48 (n=164)	4 (n=164)	98 (n=81)
cacn-1 (1:500)	Wild type	0 (n=164)	0 (n=164)	2 (n=304)
	sacy-1(tn1385)	2 (n=138)	2 (n=138)	7 (n=434)
cacn-1 (1:1,000)	Wild type	0 (n=188)	0 (n=188)	1 (n=458)
	sacy-1(tn1385)	0 (n=140)	0 (n=140)	1 (n=564)

[a]RNAi clones are listed with the target gene name in italics and the dilution factor in parentheses.

[b]Number of gonad arms scored.

[c]Number of embryos scored.

ND. not determined.

SUPPLEMENTAL FIGURES AND LEGENDS

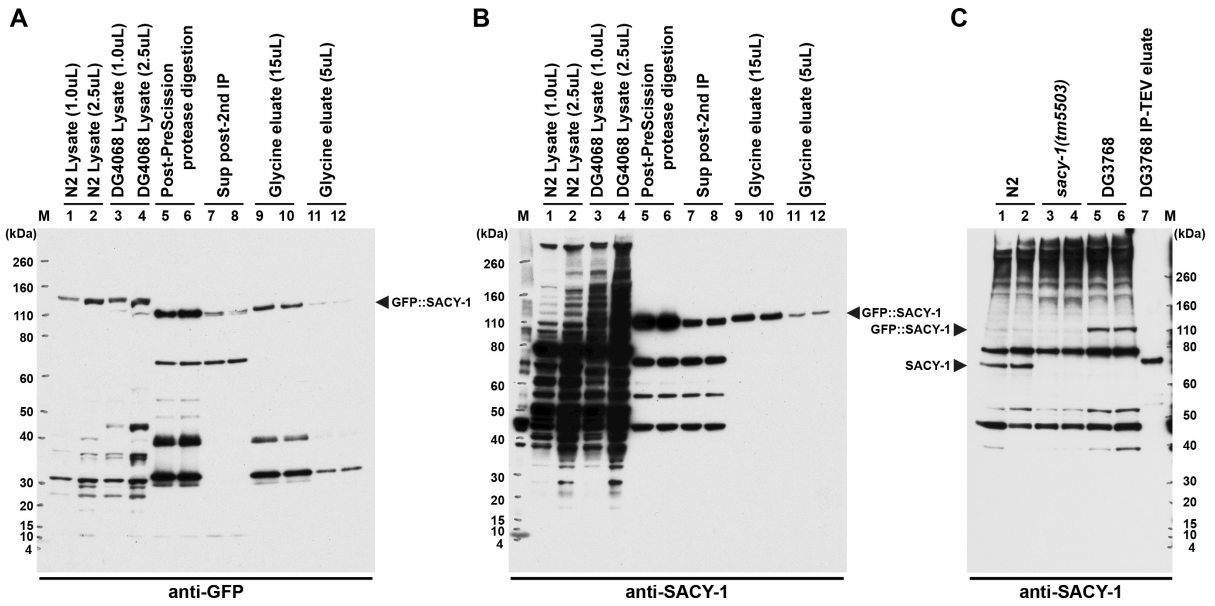

Figure S1 Tandem affinity purification of SACY-1 to identify associated proteins. (A, B) Western blot analysis of fractions from the tandem affinity purification procedure analyzed with anti-GFP (A) or R217 anti-SACY-1(411–578) antibodies (B). Note, the anti-SACY-1 antibody detects many cross-reacting bands in the lysates; however, these are removed during the purification. DG4068 is *sacy-1(tn1632[3xflag::PreScission protease site::gfp::tev::s-tag::sacy-1]) fog-1(q253*ts*)*. DG4068 was grown at 25°C from the L1 stage to generate a homogeneous population of adult females not containing embryos for the preparation of the protein lysate. (C) Affinity-purified R217 anti-SACY-1(411-578) antibody fails to detect a specific protein product in western blots of extracts from *sacy-1(tm5503)* mutants. Note, *sacy-1(tm5503)* results from a 619-bp deletion, which eliminates the second and third exons and a portion of the fourth (see Figure 4A in the main text), introducing a frame shift N-terminal to the DEAD-box domain. Importantly, the epitope detected by R217 anti-SACY-1(411-578) is C-terminal to the region deleted in *sacy-1(tm5503)*. Thus, any protein product produced from the mutant locus is predicted to lack the DEAD-box domain, consistent with the results of the western

blot. DG3768 is *sacy-1(tm5503); unc-119(ed3) tnIs102[sacy-1p::gfp::tev::s-tag::sacy-1 + Cb unc-119(+)]* III.

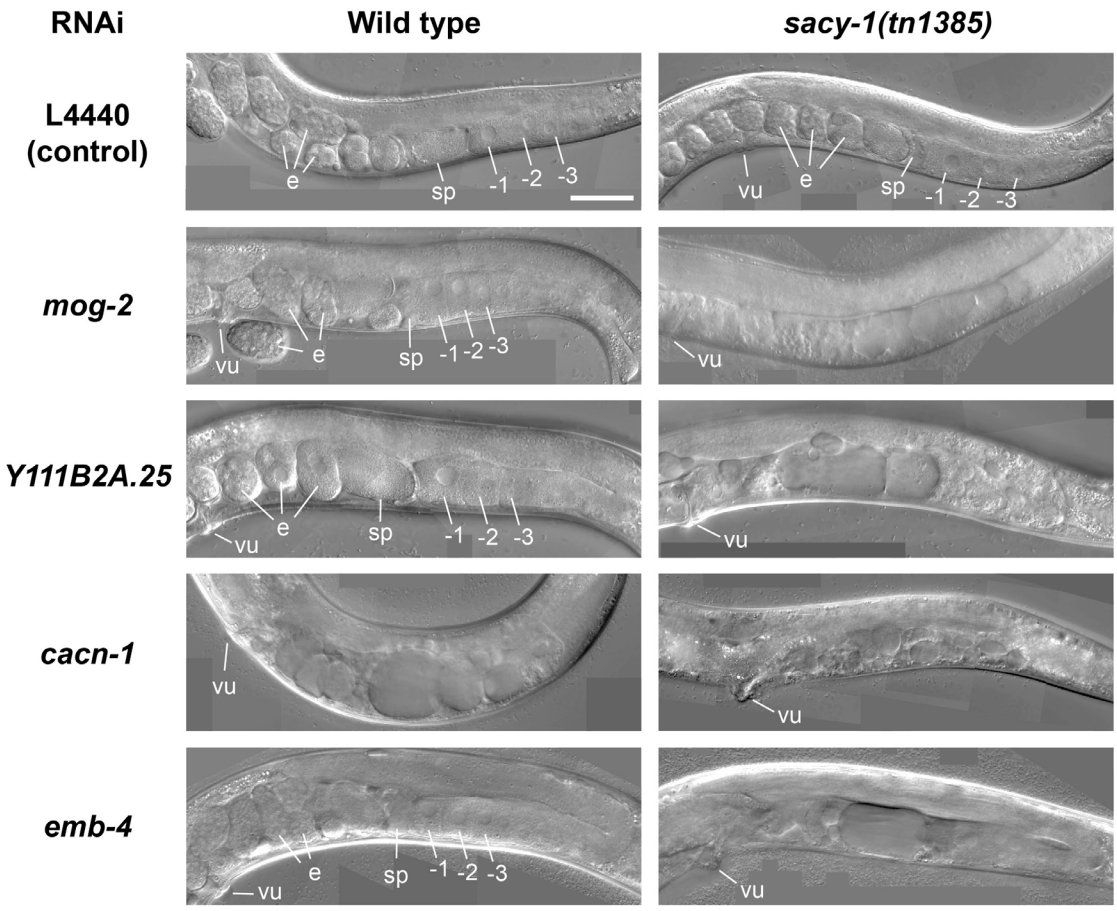

Figure S2 Gamete degeneration in *sacy-1(tn1385)* adult hermaphrodites after RNAi of *sacy-1* enhancer loci. Photomicrographs in wild-type (left panels) and *sacy-1(tn1385)* (right panels) animals following RNAi of a control (L4440 empty vector), *mog-2*, *Y111B2A.25*, *cacn-1*, and *emb-4*. RNAi of *mog-2*, *Y111B2A.25*, and *emb-4* do not induce gamete degeneration in wild-type animals. Strong *cacn-1(RNAi)* causes gamete degeneration in both *sacy-1(tn1385)* and wild-type animals, but limited *cacn-1(RNAi)* substantially enhances gamete degeneration only in *sacy-1(tn1385)* animals (see Table S7). Wild-type and *sacy-1(tn1385)* animals do not exhibit gamete degeneration after control RNAi. Embryos (e), spermatheca (sp), vulva (vu), oocytes (-1, -2, -3). Scale bar, 50 mm.

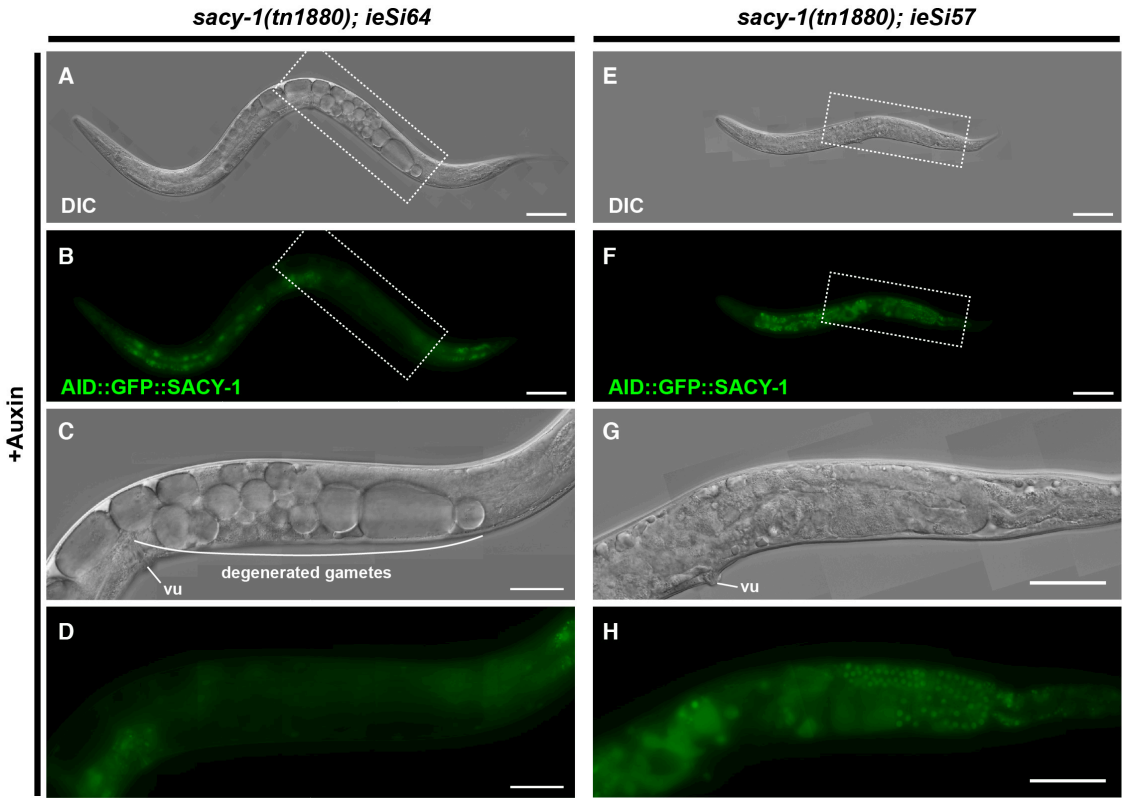

Figure S3 Use of the auxin-inducible degradation (AID) system to deplete *sacy-1(+)* activity in the germline or soma. (A–H) Use of the AID system to deplete *sacy-1(+)* in the germline (A–D) or soma (E–H) using strains containing a germline- (*ieSi64*) or soma-expressed TIR1 (*ieSi57*), respectively. Fluorescent photomicrographs (B, D, F, and H) document the auxin-dependent depletion of AID::GFP::SACY-1 in the germline (B and D) or soma (F and H). Depletion of AID::GFP::SACY-1 in the germline commencing at the L3 stage was capable of phenocopying the null mutant phenotype in a small fraction of the treated animals (C). Depletion AID::GFP::SACY-1in the soma caused slow growth and sterility (E and G). The regions within the dotted rectangles are magnified as shown. Vulva (vu). Bars, 100 µm in panels (A, B, E, and F); 50 µm in panels (C, D, G, and H).

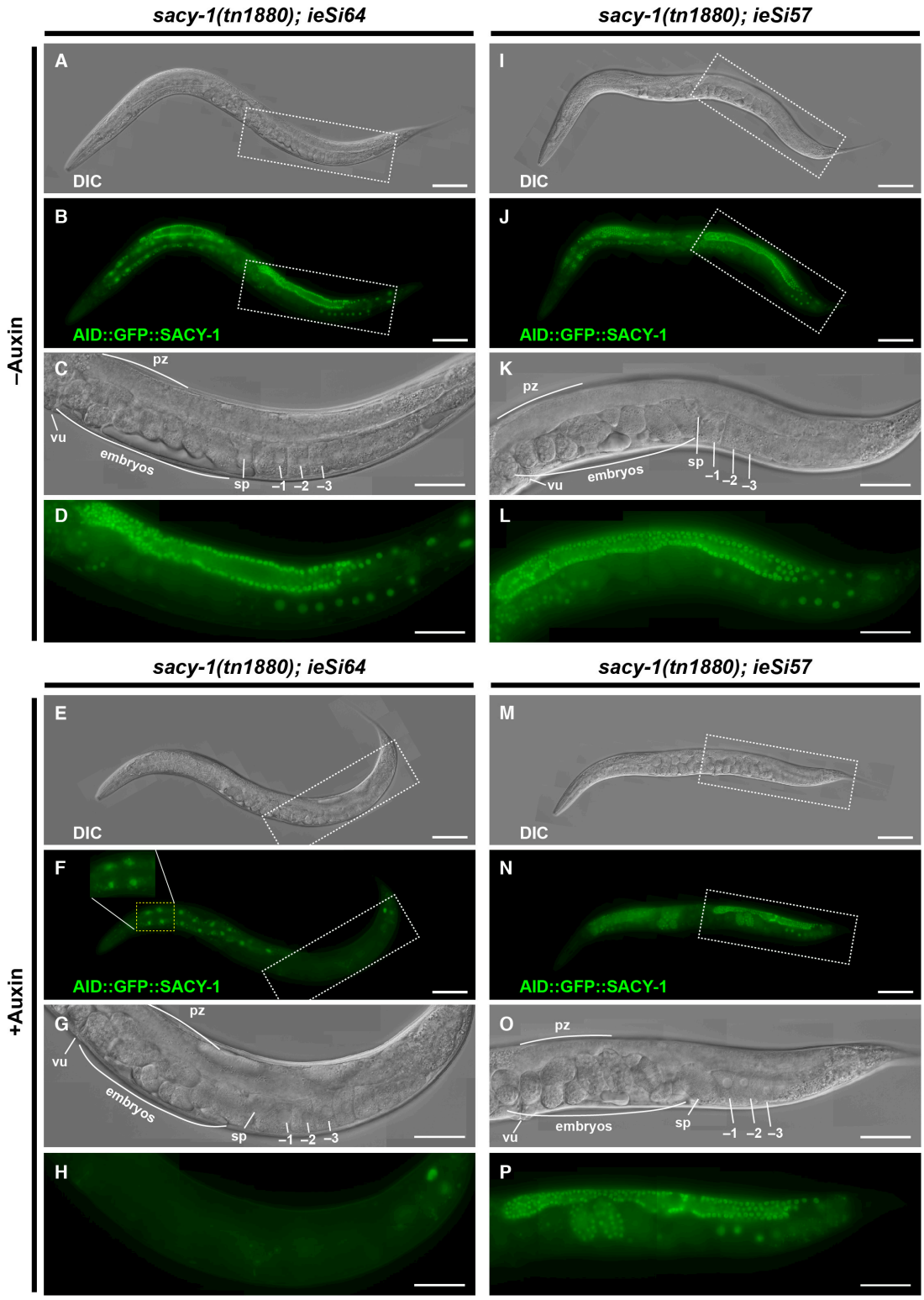

Figure S4 Depletion of SACY-1 in the germline or soma using the auxin-inducible degradation system. (A) AID::GFP::SACY-1 is depleted from the germline but not the soma using the DG4700 *sacy-1(tn1880[aid::gfp::myc::sacy-1])*; *ieSi64[gld-1p::TIR1::mRuby::gld-1 3'UTR + Cb unc-119(+)]*

strain, which expresses TIR1::mRuby in the germline. (B) AID::GFP::SACY-1 is depleted from the soma but not the germline using the DG4703 *sacy-1(tn1880[aid::gfp::myc::sacy-1])*; *ieSi57[eft-3p::TIR1::mRuby::unc-54 3'utr + Cb unc-119(+)]* strain, which expresses TIR1::mRuby in the soma. Animals were cultured on NGM medium containing 2 mM auxin for 24 hours before imaging GFP fluorescence. Oocytes (–1, –2, –3), proliferative zone (pz), spermatheca (sp), vulva (vu). The regions within the dotted rectangles are magnified as indicated. Bars, 100 μm in panels (A, B, E, F, I, J, M, and N); 50 μm in panels (C, D, G, H, K, L, O, and P).

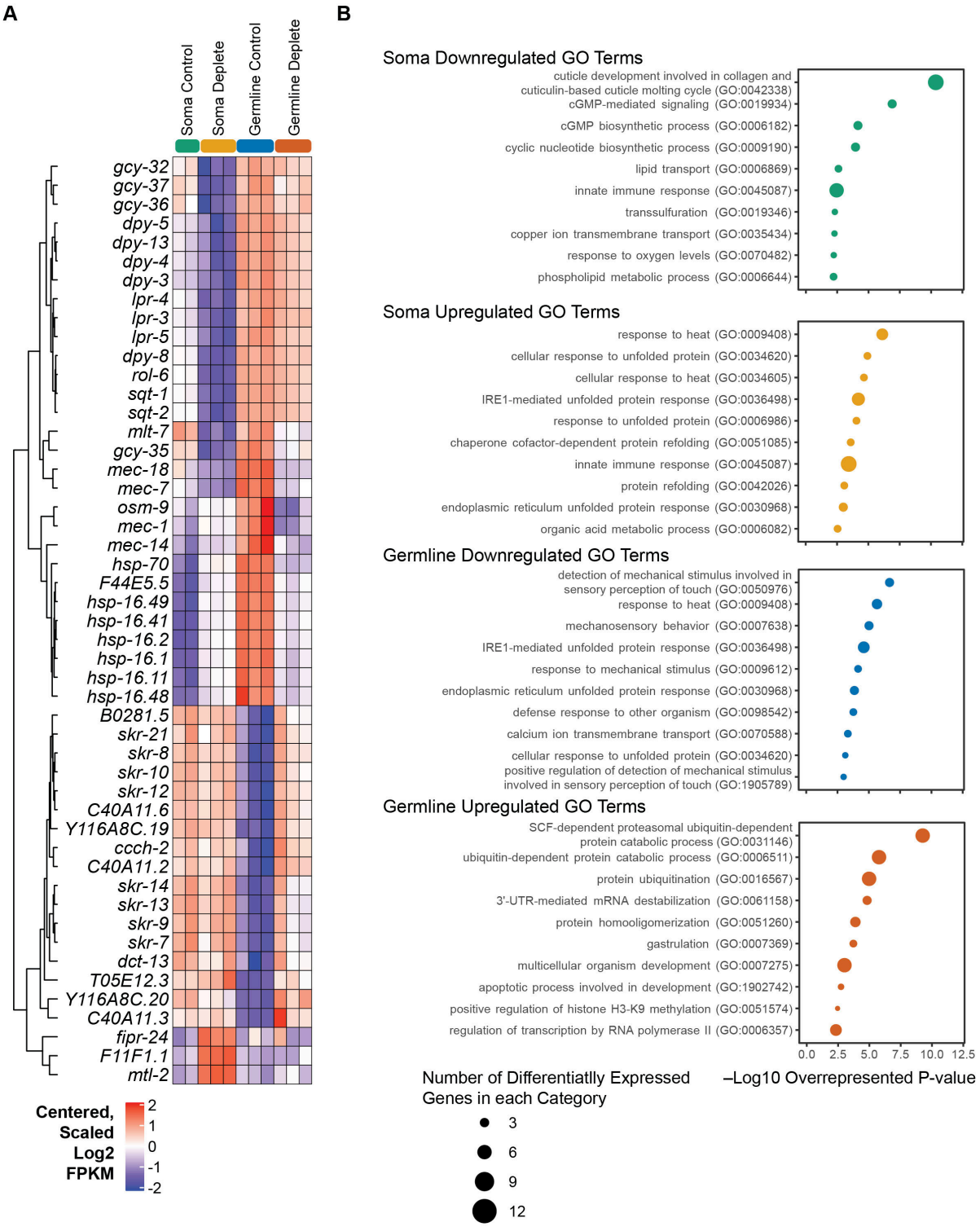

Figure S5. Changes in gene expression following SACY-1 depletion in the germline or soma. (A) Heat map of centered and scaled log2 FPKM values for transcripts that change following SACY-1 depletion in the soma or germline. Genes were selected based on the top 5 GO categories for each gene

subset in (B). The individual biological replicates are indicated at the top of (A) for the controls (green and blue bars) and the experimental samples (gold and red bars). (B). The –log10 p values for the top GO terms enriched in the SACY-1 depleted samples in the germline and the soma are indicated for upregulated (2-fold; $p<0.05$, FPKM deplete > 2.5 and mean counts > 25) and downregulated (2-fold; $p<0.05$, FPKM control > 2.5 and mean counts > 25) genes. The number of differentially expressed genes in each category is represented as the size of the circle as indicated in the legend in (B).

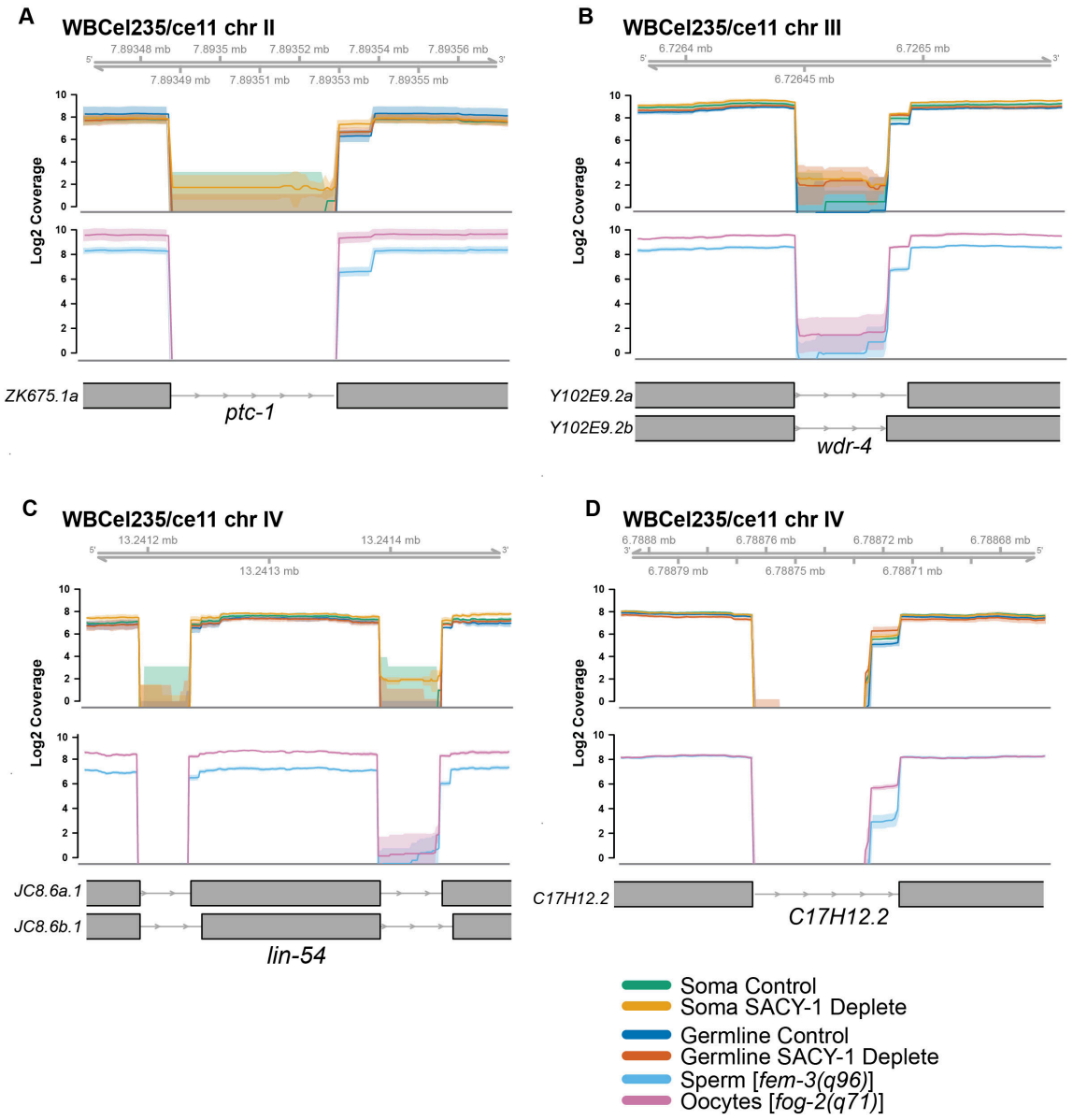

Figure S6. Examples of germline sex-specific splicing patterns affected by SACY-1 depletion. Coverage for *ptc-1* (A), *wdr-4* (B), *lin-54* (C) and *C17H12.2* (D) are shown for control (soma=green, germline=blue) and SACY-1 deplete (soma=gold, germline=red) datasets (upper panel). The data for *fog-2(q71)* (pink) and *fem-3(q96*) (cyan), which respectively have feminized and masculinized germlines, are from Ortiz *et al*. (2014) (lower panel). Alternate splice sites for *wdr-4* and *lin-54* are annotated in Ensembl release 97 as alternative transcript isoforms (gray boxes) but the alternative

splicing events are not annotated for *ptc-1* and *C17H12.2.* The solid lines represent the mean of the biological replicates and shaded regions represent the corresponding confidence interval.

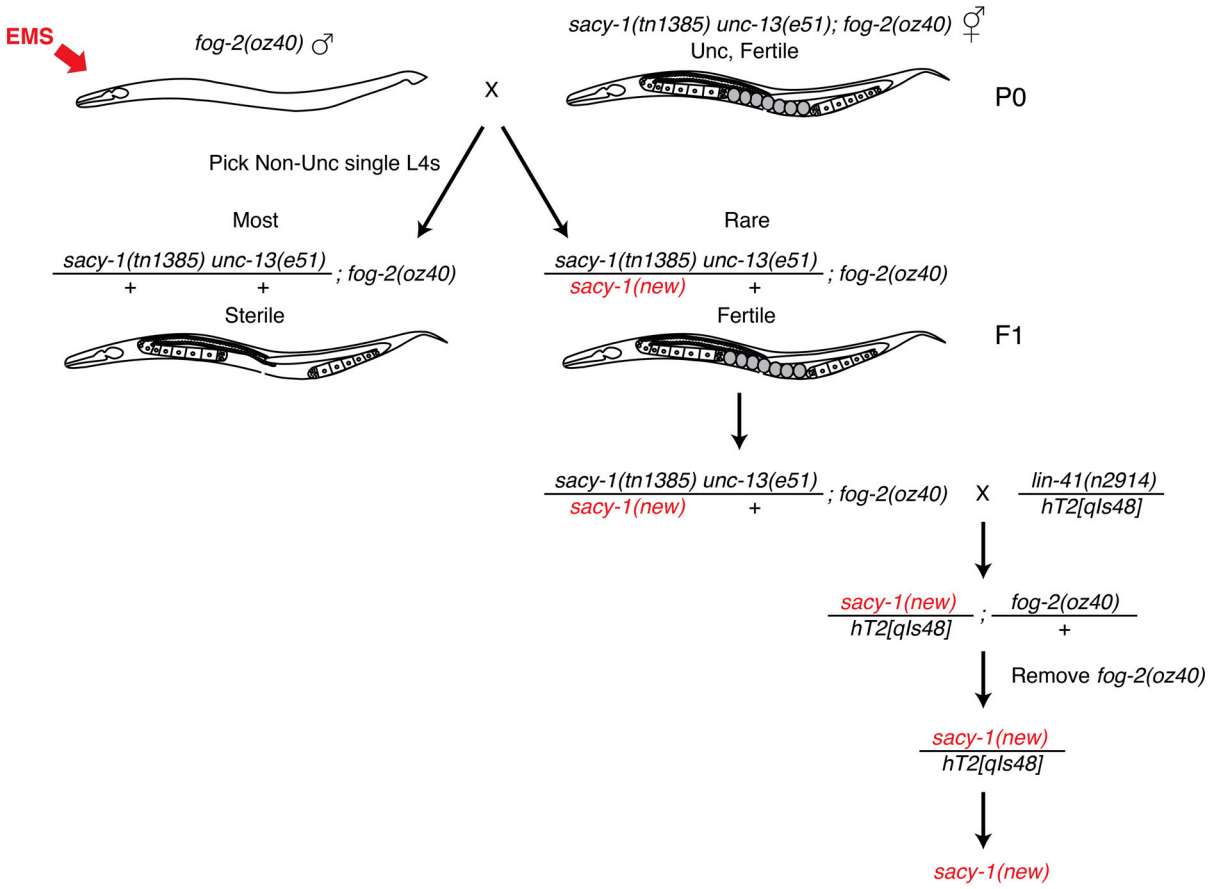

Figure S7 Schematic illustration of the genetic non-complementation screen for new *sacy-1* alleles that suppress the self-sterility of *fog-2(oz40)* null mutants, resulting from a feminization of germline phenotype. All new ethyl methanesulfonate (EMS)-induced alleles reported in this work (*tn1479*, *tn1480*, *tn1481*, *tn1482*, and *tn1483*) were generated using this method.

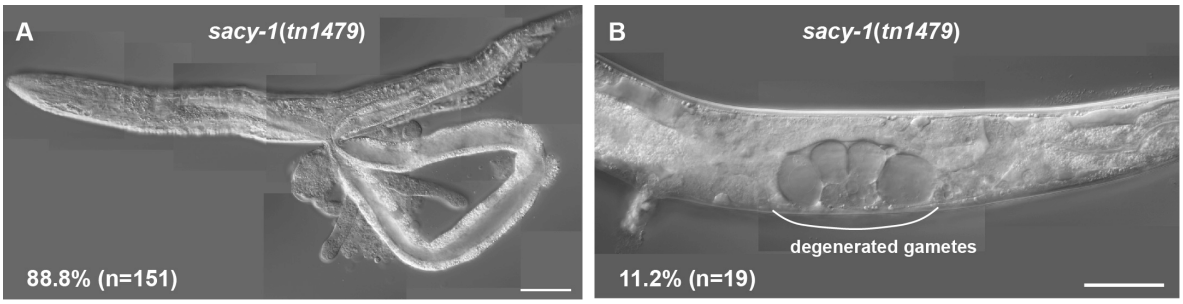

Figure S8 Phenotypes of *sacy-1(tn1479)* mutants. (A) Lethal vulval rupture phenotype, which is the predominant phenotype displayed by *sacy-1(tn1479)* homozygotes (~89%; see Table 5 in the main text). (B) Germline degeneration phenotype, which is characteristic of *sacy-1* null alleles. Approximately 11% of *sacy-1(tn1479)* homozygotes display this phenotype (see Table 5 in the main text). Bars, 50 μm.

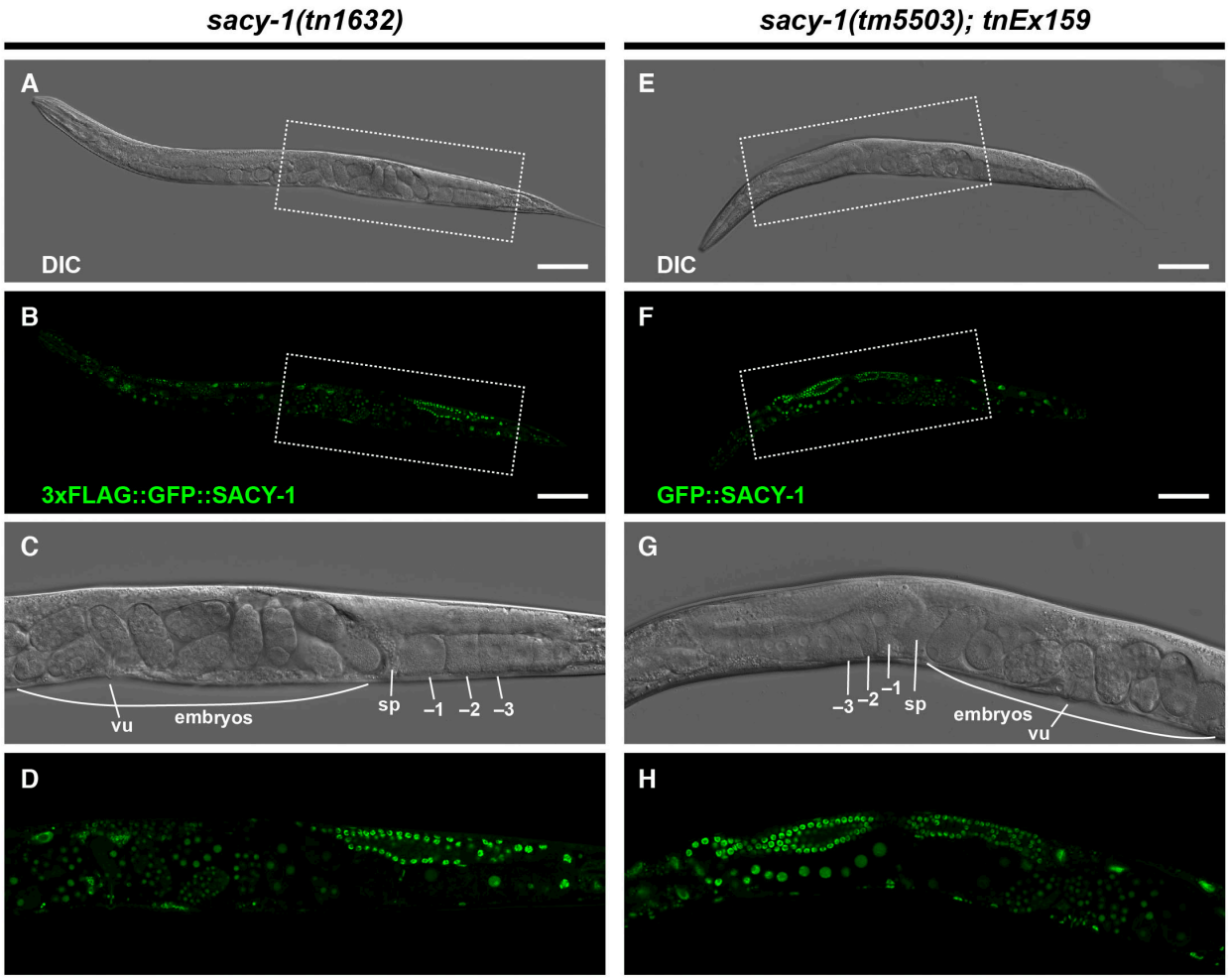

Figure S9 The extrachromosomal array *tnEx159* expresses GFP::SACY-1 in the germline and soma at wild-type levels. (A, C, E, and G) DIC images of DG4070 *sacy-1(tn1632)* (A and C) and DG3485 *sacy-1(tm5503); tnEx159* adults (E and G). Accompanying fluorescent images are shown in (B, D, F, and H). The regions within the dotted rectangles are magnified as indicated. *sacy-1(tn1632)* is a CRISPR-Cas9-induced allele in which 3xFLAG::GFP sequences are fused to the N-terminus of SACY-1.Bars, 100 µm. Embryos, oocytes (–1, –2, and –3), the spermatheca (sp), and the vulva (vu) are indicated.

DESCRIPTION OF SUPPLEMENTAL FILES

File S1. Identification of SACY-1-associated proteins by affinity purification and mass spectrometry.

File S2. Gene expression and splicing alternations following SACY-1 depletion in the germline and soma.

File S3. Genes exhibiting germline sex-specific splicing patterns in the data of Ortiz *et al*. (2014).

SUPPLEMENTAL REFERENCES

Chaudhary, N., C. McMahon, and G. Blobel, 1991 Primary structure of a human arginine-rich nuclear protein that colocalizes with spliceosome components. Proc. Natl. Acad. Sci. USA 88: 8189–8193.

Fabrizio, P., J. Dannenberg, P. Dube, B. Kastner, H. Stark *et al*., 2009 The evolutionarily conserved core design of the catalytic activation step of the yeast spliceosome. Mol. Cell 36: 593–608.

Grainger, R. J., and J. D. Beggs, 2005 Prp8 protein: at the heart of the spliceosome. RNA 11: 533–557.

Hastings, M. L., E. Allemand, D. M. Duelli, M. P. Myers, and A R. Krainer, 2007 Control of pre-mRNA splicing by the general splicing factors PUF60 and U2AF^{65}. PLoS One 2: e538.

Kao, H.-Y., and P. G. Siliciano, 1996 Identification of Prp40, a novel essential yeast splicing factor associated with the U1 small nuclear ribonucleoprotein particle. Mol. Cell. Biol. 16: 960–967.

Keikhaee, M. R., E. B. Nash, S. M. O'Rourke, and B. Bowerman, 2014 A semi-dominant mutation in the general splicing factor SF3a66 causes anterior-posterior axis reversal in one-cell stage *C. elegans* embryos. PLoS One 9: e106484.

Li, X., S. Liu, J. Jiang, S. Espinosa, R. C. Hill *et al*., 2017 CryoEM structure of *Saccharomyces cerevisiae* U1 snRNP offers insight into alternative splicing. Nat. Commun. 8: 1035.

Longman, D., I. L. Johnstone, and J. F. Cáceres, 2000 Functional characterization of SR and SR-related genes in *Caenorhabditis elegans*. EMBO J. 19: 1625–1637.

Page-McCaw, P. S., K. Amonlirdviman, and P. A. Sharp, 1999 PUF60: a novel U2AF65-related splicing activity. RNA 5: 1548–1560.

Schneider, M., H.-H. Hsiao, C. L. Will, R. Giet, H. Urlaub *et al*., 2010 Human PRP4 kinase is required for stable tri-snRNP association during spliceosomal B complex formation. Nat. Struct. Mol. Biol. 17: 216–221.

Will, C. L., H. Urlaub, T. Achsel, M. Gentzel, M. Wilm *et al*., 2002 Characterization of a novel SF3b and 17S U2 snRNP proteins, including a human Prp5p homologue and an SF3b DEAD-box protein. EMBO J. 18: 4978–4988.

Zhang, X., C. Yan, J. Hang, L. I. Finci, J. Lei *et al.*, 2017 An atomic structure of the human spliceosome. Cell 169: 918–928.